ACOUSTICAL AND FLOWFIELD CHARACTERIZATION OF A TABLETOP ROCKET MOTOR

Max Kandula, Ravi Margasahayam
Dynacs Inc., John F. Kennedy Space Center, FL, U.S.A.

Michael P. Norton
University of Western Australia, Crawley, Western Australia

Raoul E. Caimi
NASA John F. Kennedy Space Center, FL, U.S.A.
E-mail address: max.kandula-1@ksc.nasa.gov

Abstract

An analysis of the acoustical and flowfield environment for the scaled 1-pound-force (lbf) thrust tabletop motor was performed. The jet characterization is based on computational fluid dynamics (CFD) in conjunction with Kirchhoff surface integral formulation and compared with correlations developed for measured rocket noise and a pressure fluctuation scaling (PFS) method. Comparisons are made for the overall sound pressure levels (OASPL's) and spectral dependence of sound pressure level (SPL).

INTRODUCTION

At NASA Kennedy Space Center, a Launch Systems Testbed (LST) is currently under development to establish a capability to simulate small-scale launch vehicle environment for use in testing and evaluation of launch pad designs for future space vehicles. These prediction methods include computational fluid dynamics (CFD), analytical correlations, and pressure fluctuation scaling (PFS) methods. This report, primarily derived from [1], summarizes the analytical studies of a small-scale tabletop rocket that is being acquired from NASA Stennis Space Center for the purpose of establishing the initial test facility and instrumentation.

DESCRIPTION OF THE TABLETOP ROCKET

Fig. 1 shows a schematic of the nozzle geometry for the tabletop motor [2]. This motor has cylindrical Plexiglas fuel burning in gaseous oxygen. The combustion gas is approximated as carbon dioxide (CO_2). The nozzle exit conditions, as derived form isentropic expansion [3] are shown in Table 1.

ANALYSIS

CFD/Kirchhoff Analysis

The CFD/Kirchhoff analysis is based on the application of OVERFLOW CFD Navier-Stokes code [4, 5] for identifying the noise sources in the nonlinear source field and Kirchhoff surface integral [6] for the propagation of sound radiation to the near field and the far field. For the acoustic radiation, the Kirchhoff code YORICK [7] was considered.

CFD Solution. For the CFD computations, an axisymmetric grid of 200 x 100 is considered. The CFD solution converged after about 15,000 time-step iterations (the code is run in a time-accurate manner) before a periodic state is established.

Acoustic Solution. After a periodic state is established, the data from CFD is communicated to the Kirchhoff code. The radius of the Kirchhoff surface is taken 6 radii from the jet axis.

Correlation/Analytical Method

Leneman [8] proposed an empirical correlation for the OASPL as

$$\mathrm{OASPL\,(dB)} = 115 + 10\,\log(F\,I) - 20\log(x) \tag{1a}$$

where F denotes the total thrust (lbf), I the specific impulse (sec), and x the axial distance (ft) in the far field from the jet exit plane. Margasahayam and Caimi [9] proposed as:

$$\mathrm{OASPL\,(dB)} = 115 + 10\log(F\,I) - 20\log(x) - 20\times 10^{(-x/50)} \tag{1b}$$

with the fourth term providing a near-field correction to the Leneman correlation.

The NASA SP-8072 method [10] represents a more accurate correlation compared to the Leneman correlation and is based on normalized relative power spectrum from test data.

Pressure Fluctuation Scaling Method

In the method of pressure fluctuation scaling due to Norton et al. [11], which has been successfully used for industrial gas piping networks, etc., the nondimensional fluctuating pressure spectral density Φ_p is given by

$$\Phi_p(\Omega) = \frac{4G_p(\omega)}{\rho^2 U^3 a}, \quad \Omega = \omega a / U \tag{2}$$

where Ω is the nondimensional frequency (Strouhal number), G_p is the fluctuating pressure spectral density, ρ is the gas density, U is the flow velocity, a is the nozzle exit radius, and $\omega = 2\pi f$. The turbulent wall pressure spectrum (shell or flat plate) provides a lower level, and the severe internal flow disturbance provides the upper level for scaling purposes.

The sound spectrum is then calculated at the exit downstream of the shock. Power spectral estimates of fluctuating pressure for the tabletop rocket are obtained from

$$S_p(\omega) = \frac{\Phi_p(\Omega)\rho^2 U^3 a \Delta\omega_i}{4}, \quad \omega_i = U\Omega_i / a \tag{3}$$

where $\Delta\omega_i$ is the nominal bandwidth of band i with center frequency ω_i. Correction factors are then applied for the open jet exhausting out of the nozzle. At this stage, a $1/r$ (r is the distance from the sound source) decay with distance from the nozzle is assumed for circumferential radiation away from the exit plane (e.g., position A, Fig. 1). The $1/r$ decay is also considered for post shock centerline decay (e.g., position X) because the mean flow will enhance/convect the monopole- and dipole-type radiation from the duct exit. These assumptions need to be refined.

RESULTS AND COMPARISON

Flowfield Results

The axial variation of Mach number at the centerline (Fig. 2) indicates that the core length of the jet extends to about 25 jet radii from the exit plane. The average Mach number in the core region downstream of the shock is about 0.6, characterizing the jet as subsonic.

Acoustical Results

Table 2 summarizes the comparison of OASPL at stations A, E, and X (Fig. 1) as estimated by the different methods.

The spectral composition of 1/3 octave SPL at point A in the exit plane is presented in Fig. 3a. The SPL from the upper-level PFS exceeds the CFD result. However, both the CFD and the upper-level PFS method suggest a peak frequency of about 20 kilohertz (kHz), which corresponds to a Strouhal number St = 0.20. The lower-level PFS method produces SPL that is close to that of the CFD but produces a peak frequency of about 100 kHz, which appears somewhat overestimated.

A comparison of the 1/3 octave SPL content at location E on the axis downstream of the exit plane is portrayed in Fig. 3b. In general, the SPL values at E are considerably higher than those at position A, due to the near-field location of E and the effect of directivity. A peak frequency of about 35 kHz (corresponding to St = 0.35) is indicated by CFD, the NASA-SP method, and the PFS upper-level method. The CFD results for the SPL are higher than those from the NASA-SP method. In the case of the PFS method, the upper-level values for the SPL are closer to the CFD, whereas the lower-level results match well with the NASA-SP method.

Fig. 3c compares the spectral distribution of 1/3 octave SPL at location X, which is downstream of location E but 1 jet radius away from the axis. In general, the sound pressure levels at X are smaller than those at E. A reduced peak frequency of about 25 kHz (corresponding to St = 0.25), relative to location E, is indicated by CFD, the NASA-SP method, and the PFS upper-level method. The SPL variation between the various methods at position X is somewhat smaller compared to that at positions A and E.

A comparison of the 1/3 octave SPL at locations A, E, and X as predicted by CFD is shown in Fig. 4. Downstream of the exit plane, the peak frequency level is increased in the near field, as the distance from the exit plane is decreased. While there appears to be a similarity in the shape of the SPL spectrum between E and X, there is a departure in similarity at position A for frequencies in excess of about 40 kHz, where a rapid decline in SPL is observed. This lack of similarity in the SPL spectrum at position A is perhaps attributable to the existence of a normal shock near the nozzle exit or to the far-field directivity effects.

CONCLUSIONS

The CFD/Kirchhoff method provided flowfield structure and distributions of the OASPL and SPL spectrum for the tabletop rocket. Because of the very small size of the nozzle exit diameter, the jet is distinguished by high peak frequency levels (20 to 35 kHz) for the SPL spectrum. A comparison of the results from CFD, the NASA-SP method, and the PFS method at three spatial locations (A, E, and X) showed that a similarity in shape is generally noted for the SPL composition. There is some disagreement between the different methods for the peak frequencies and the SPL values. A more realistic assessment of these methods can only be carried out with the aid of an experimental test program currently under development.

ACKNOWLEDGEMENT

The authors are greatly indebted to Dr. William St. Cyr of the Propulsion Directorate of NASA Stennis Space Center for providing the tabletop rocket model for testing purposes. In addition, the authors wish to thank Robert Field of NASA Stennis Space Center for providing data on the tabletop rocket motor and useful discussions and Dr. Denis Karczub of SVT-Engineering Consultants in Western Australia for assistance with the pressure fluctuation scaling method. Thanks are due to Dr. Pieter Buning of NASA Langley Research Center for discussions with regard to the OVERFLOW code and to Geoffrey Rowe of Dynacs Inc. for assistance in the spectral decomposition of CFD data. Thanks are also due to Stanley Starr, Chief Engineer, Dynacs Inc., for providing a detailed review of the manuscript.

REFERENCES

1. Kandula, M., Margasahayam, R., Norton, M.P., and Caimi, R., Acoustical and Flowfield Characterization of a Scaled Tabletop Rocket, NASA TM-210262 (2001)

2. Field, R., NASA Stennis Space Center, Personal Communication (2001)

3. Shapiro, A.H., *The Dynamics and Thermodynamics of Compressible Fluid Flow*, Vol. 1. (John Wiley & Sons, New York, 1953)

4. Buning, P.G., Jesperson D.C., Pulliam, T.H., Chan, W.M., Slotnick, J.P., Krist, S.E., and Renze, K.J., OVERFLOW User's manual - version 1.8, NASA Langley Research Center (1998)

5. Kandula, M. and Caimi, R., Simulation of Jet Noise with OVERFLOW CFD Code and Kirchhoff Surface Integral, AIAA 2002-2602, 8th AIAA/CEAS Aeroacoustics Conference, Breckenridge, Colorado (2002)

6. Kirchhoff, G.R., Zur Theorie der Lichtstrahlen, Annalen der Physik und Chermie, **18**, 663-695, 1883

7. Pilon, A.R. and Lyrintzis, A.S., Development of an Improved Kirchhoff Method for Jet Acoustics, AIAA J., **37**, 783-790 (1998)

8. Leneman, G., Determination of Maximum Ground Noise During a Rocket Launch – Discussion and Simple Prediction Method, Proceeding of the Institute of Environmental Sciences (1973)

9. Margasahayam, R. and Caimi, R., Rocket Noise Prediction Program – Application, 7th International Congress on Sound and Vibration, Garmisch-Partenkirchen, Germany (2000)

10. Anonymous, Acoustic Loads Generated by the Propulsion System, NASA-SP-8072 (1971)

11. Norton, M.P., *Fundamentals of Noise and Vibration Analysis*. (Cambridge University Press, 1989)

Table 1. Summary of Nozzle Parameters

Parameter	Value
Stagnation pressure, psia	54.7
Stagnation temperature, °R	1960
Nozzle mass flow rate, lbm/s	0.0247
Nozzle throat diameter, inch	0.2
Exit pressure, psia	2.38
Exit temperature, °R	987
Exit velocity, ft/s	3,170
Nozzle exit Mach number	2.65
Nozzle exit density, lbm/ft^3	0.0099
Jet exit Reynolds number	2.9×10^4

Table 2. Comparison of OASPL at Locations A, E, and X

Location	CFD	Leneman		NASA-SP 8072	PFS	
		Original	Modified		Upper Level	Lower Level
A	118	–*	–	–	153	119
E	151	175	155	125	176	130
X	140	144	124	117*	135	122

* Not applicable, ** Value corresponding to $z = 0$

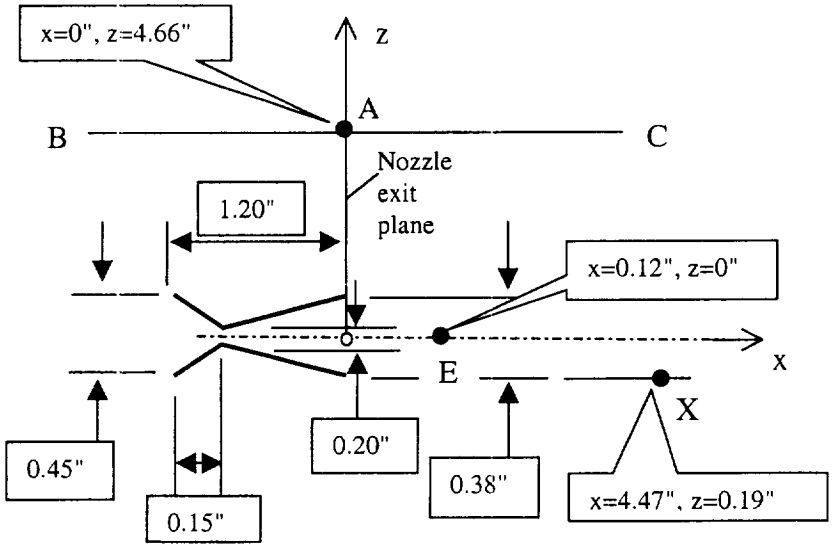

Fig. 1. Schematic of the Tabletop Rocket Nozzle

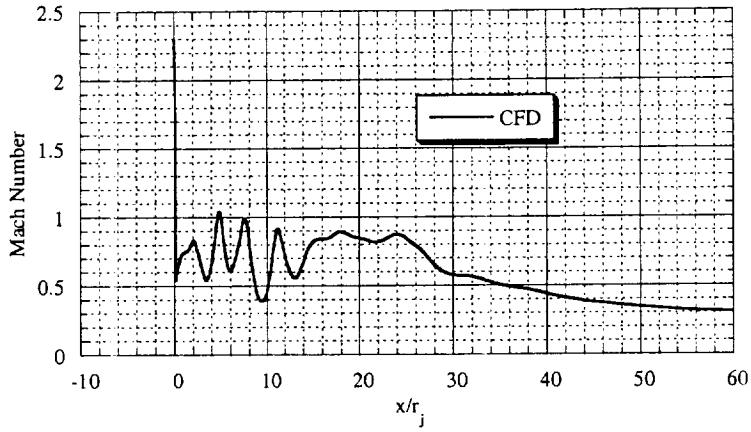

Fig. 2. Jet Centerline Variation of Mach Number From CFD

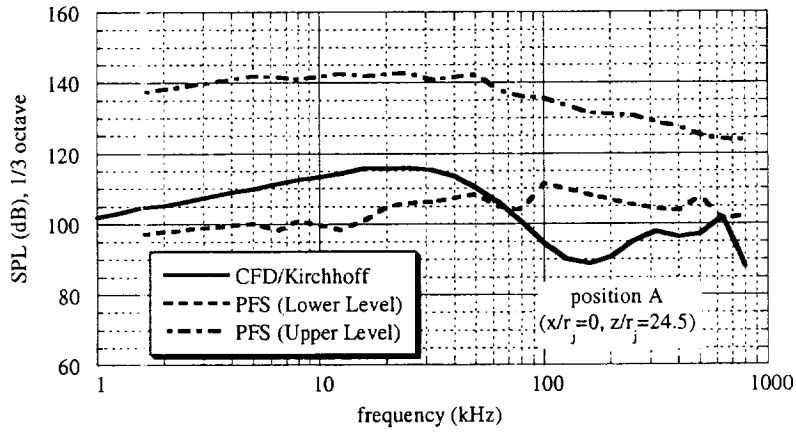

Fig. 3a. Comparison of 1/3 Octave Spectra at Location A

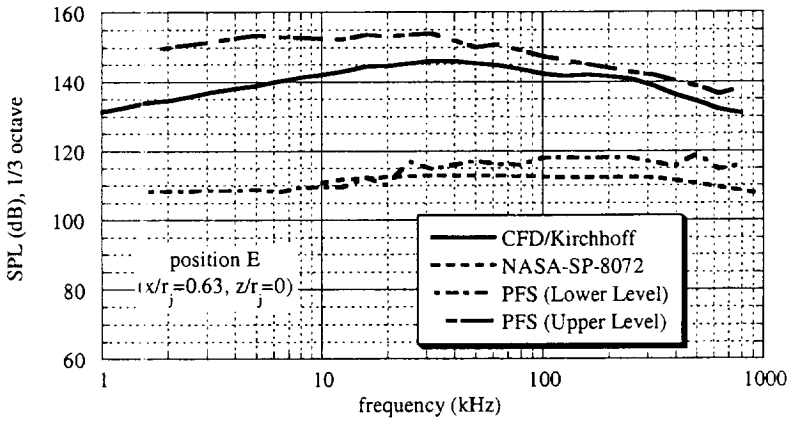

Fig. 3b. Comparison of 1/3 Octave SPL Spectra at Location E

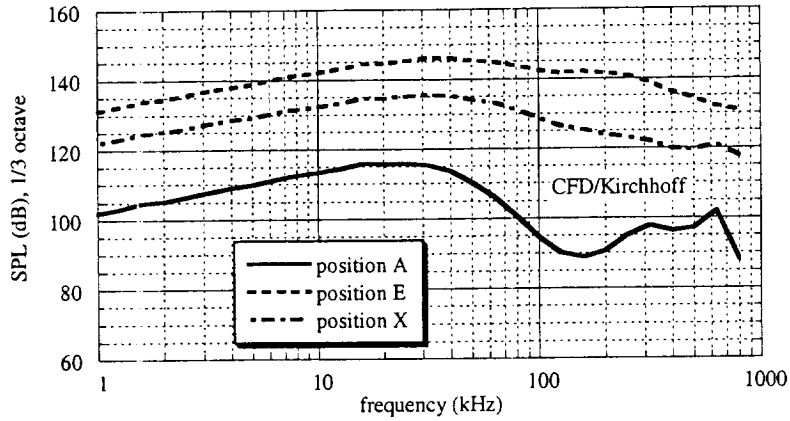

Fig. 3c. Comparison of 1/3 Octave SPL Spectra at Location X

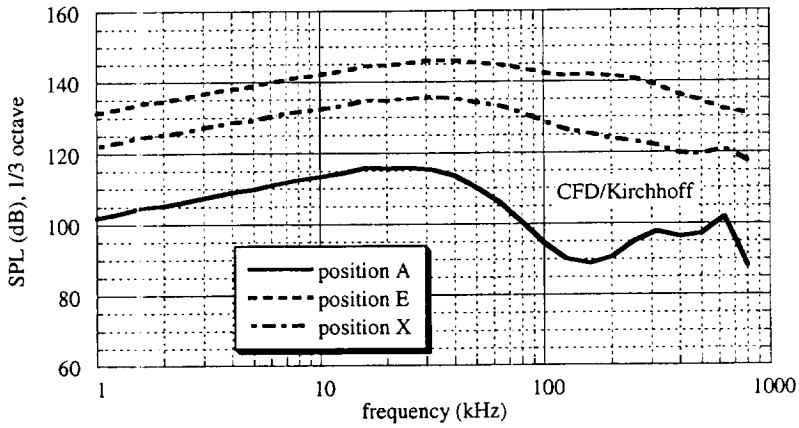

Fig. 4. Comparison of 1/3 Octave SPL Spectra From CFD at A, E, and X